Because of this instrumental asymmetry, it was decided to perform a second experiment with a pair of cadmium plates, where it was hoped that lesser asymmetry would be encountered. Because the absorption cross section for Cd is much larger than that for LiF, a much thinner plate is needed to attain the optimum e^{-1} transmission. This in turn means that the intrinsic phase angle introduced by passage of neutrons through the Cd plate is reduced to 132°, about 35 times smaller than that encountered with the LiF plates. It follows that less control of the thickness equivalence of two plates is called for in minimizing intrinsic phase differences. Accordingly, a thin sheet of cadmium was cold rolled to the desired thickness (0.086 mm) and various sections were studied by neutron transmission. Selected sections were then cut and mounted on picture-frame holders for use in the interferometer. Plates A and B gave transmission values of 0.378 55 and 0.378 94, respectively, with an uncertainty of 0.000 43.

A package of interferometer data was then obtained with the Cd plates in the same manner as in the LiF experiment, again with plate interchange, and the results are summarized in the lower section of Table I. The results for Cd indicate that the intrinsic plate asymmetry is now much reduced from that encountered in the first experiment and also that the Shimony phase angle Δ is again less than 1 standard deviation. Interpreting the results of the Cd-attenuator experiment in terms of Eq. (3), we obtain

$$b=(+2.3\pm 2.9)\times 10^{-13}\ \text{eV}.$$

Combining the results of the two experiments, we obtain

$$b(\text{total data})=(+1.1\pm 2.3)\times 10^{-13}\ \text{eV}.$$

This establishes an upper limit on the magnitude of the nonlinear term in Eq. (1) (Ref. 4) which is about three orders of magnitude smaller than the upper limit value of 4×10^{-10} eV implied by the Lamb-shift experiments. It may be noted that the sensitivity attained in the present experiment implies that the interferometer technique can be exploited to measure very small energy modifications of a neutron beam on the order of 10^{-13} eV.

We should like to express our appreciation to Professor A. Shimony and Professor D. M. Greenburger for many helpful conversations during the course of the experiment and to A. D'Addario for his skilled craftsmanship in constructing the interferometer assembly. This work was supported by the National Science Foundation and the U. S. Department of Energy.

[a]Permanent address: Stonehill College, North Easton, Mass. 02356.

[1]A. Shimony, Phys. Rev. A 20, 394 (1979).

[2]I. Bialynicki-Birula and J. Mycielski, Ann. Phys. (N.Y.) 100, 62 (1976).

[3]A. Zeilinger, C. G. Shull, M. A. Horne, and G. L. Squires, in *Proceedings of the International Conference, Grenoble, 1978,* edited by U. Bonse and H. Rauch (Oxford Univ. Press, Oxford, England, 1980).

[4]From the data obtained we are unable to make any interesting statements about limits on the magnitude of a general nonlinear term $F(|\psi|^2)\psi$, unless the form of the function F is specified and unless the absolute magnitude of $|\psi|^2$ is known.

Attenuation and Recombination of Quarks in Nuclear Matter

Arnon Dar and Fujio Takagi[a]
Department of Physics, Technion–Israel Institute of Technology, Haifa, Israel
(Received 22 May 1979)

Quark models of hadron production in the beam-fragmentation region are extended to production off nuclei by taking into account quark attenuation in nuclear matter. Simple expressions are derived for the A dependence of the production of beam fragments. They reproduce well the experimental data on hadron-nucleus and virtual-photon–nucleus collisions.

Recent experimental studies of interactions of high-energy leptons[1] and hadrons[2] with nuclear targets have confirmed previous observations[3] of a nuclear attenuation in nondiffractive production of hadrons with large x and small p_T.

In this Letter we include quark attenuation in nuclear matter in the standard quark models[4] of hadron production and derive simple expressions for the A dependence[5] of hadron production at large x and small p_T. The expressions are independent of the details of the hadronization mechanism, have no free parameter, and describe re-

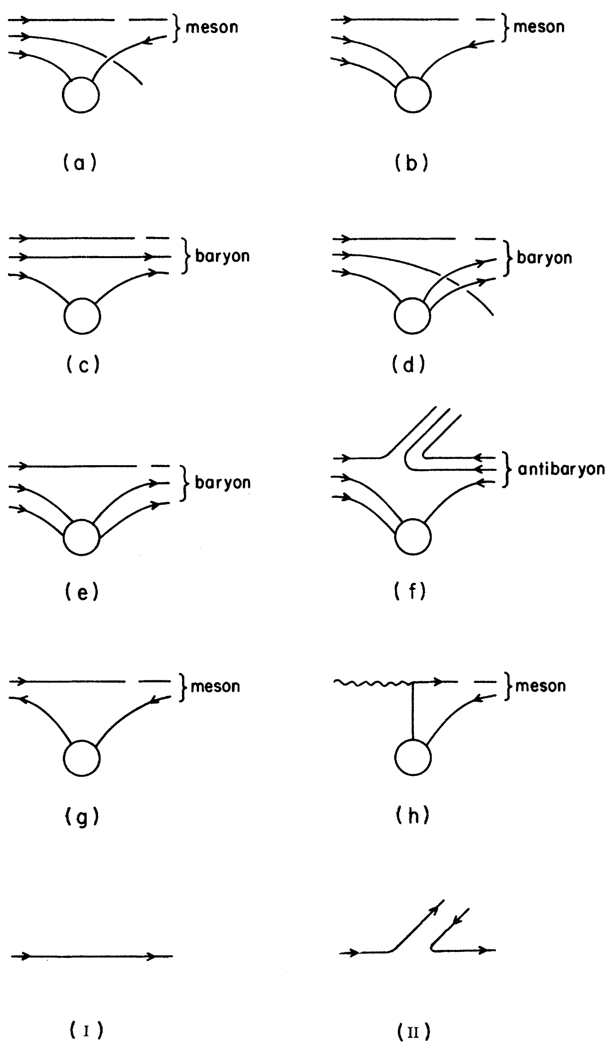

FIG. 1. Quark diagrams for large-x and small-p_T production of (a), (b) mesons, (c)–(e) baryons, and (f) antibaryons in baryon-nucleus collisions, of mesons in meson-nucleus collisions, and of mesons in virtual-photon– (or intermediate weak boson) nucleus collisions. The broken lines with arrow at the top of each diagram [(a)–(h)] stand for (I) in case of combination and for (II) in case of fragmentation.

markably well the observed nuclear attenuation.[6]

We adopt the following quark picture of production of hadrons with large x and small p_T: During the collision, valence quarks of the projectile either collide with target nucleons and are stripped off the projectile, or escape such collisions and retain their original fraction x of the incident momentum.[7] Quark(s) with large x that escape collisions, which we call leading quark(s), can hadronize by recombining with slow quark(s) ($x\sim 0$) either newly produced or already present in the target or in the beam, as in the recombination models. They can also emit a slow fragment and then recombine, as in the quark fragmentation/cascade models.[8] In both cases a hadron is produced with approximately the same x as that of the leading quark(s). These mechanisms are illustrated by the quark diagrams in Figs. 1(a)–1(h).

We first argue that their A and x dependences factorize. Different x dependence for different targets can come from A-dependent momentum distributions of the quarks that recombine with the leading quarks to form the large-x hadrons. However, if we denote by x_1 and x_2 the x of the partons (quarks, antiquarks, diquarks, etc.) in the projectile and in the target, respectively, that recombine into a hadron of mass m with $x = x_1 - x_2$ $(0 \leq x_i \leq 1)$, then

$$x_i = [(-1)^{i+1}x + (x^2 + 4m^2/S^1)^{1/2}]/2, \qquad (x+x_2)x_2 = m^2/s, \tag{1}$$

where s is the square of the c.m. energy of the colliding particles. For large positive x values and high energies $(m^2/s \to 0)$, Eq. (1) requires that $x_2 \to 0$, and thus $x = x_1$ and the x distribution of the hadrons produced via a particular diagram in Fig. 1 depends only on the projectile.

Since free quarks do not seem to exist, leading quarks must hadronize before leaving the interaction region, and the sum of the probabilities of all the possible recombinations must be 1. If the relative abundance of quark flavors around $x=0$ is A independent, then the individual recombination probabilities are A independent. Hence the A dependence of the quark diagrams results only from the stripping probabilities. It can be calculated using standard "nuclear optics" techniques.[9] Let $S_{hA}(q_1, \ldots, q_j)$ denote the cross section for stripping the valence quarks $q_1, \ldots, q_j$ from the projectile when it passes through the target nucleus A. Let σ_q be the quark-nucleon total cross section ($q = u$, $\bar{u}$, $\bar{d}$, d, s, $\bar{s}$, etc.) and let $T(b)$ be the nuclear thickness at impact parameter b along the incident z direction $[T(b) = \int_{-\infty}^{\infty} \rho(\vec{b}+\vec{z})dz$, where $\int \rho(r)d^3r = A]$. With the aid of the optical relation,

$$\sigma_{xA} = \int \{1 - [1 - \sigma_{xp}T(b)/A]^A\}d^2b = \int_{A\gg 1} \{1 - \exp[-\sigma_{xp}T(b)]\}d^2b, \tag{2}$$

and the additive-quark-model relations,[10]

$$\sigma_q \cong \sigma_{\bar{q}} \cong \tfrac{1}{2}\sigma_{\pi p} \cong \tfrac{1}{3}\sigma_{pp}, \qquad \sigma_s \cong \sigma_{\bar{s}} \cong \sigma_{Kp} - \tfrac{1}{2}\sigma_{\pi p}, \tag{3}$$

it is easy to derive relations like ($q \equiv u$ or d)

$$\begin{aligned} &S_{\pi A}(q) = S_{\pi A}(\bar{q}) = \sigma_{\pi A} - \sigma_{qA},\\ &S_{\pi A}(q\bar{q}) = 2\sigma_{qA} - \sigma_{\pi A},\\ &S_{KA}(s) = S_{KA}(\bar{s}) = \sigma_{KA} - \sigma_{qA},\\ &S_{KA}(q) = S_{KA}(\bar{q}) = \sigma_{KA} - \sigma_{sA},\\ &S_{KA}(s\bar{q}) = S_{KA}(q\bar{s}) = \sigma_{sA} + \sigma_{qA} - \sigma_{KA},\\ &S_{pA}(d) = \tfrac{1}{2}S_{pA}(u) = \sigma_{pA} - \sigma_{\pi A},\\ &S_{pA}(uu) = \tfrac{1}{2}S_{pA}(ud) = 2\sigma_{\pi A} - \sigma_{pA} - \sigma_{qA},\\ &S_{pA}(uud) = \sigma_{pA} + 3\sigma_{qA} - 3\sigma_{\pi A}. \end{aligned} \quad (4)$$

The invariant cross section $\sigma_A(h \to h') \equiv E d^3\sigma(hA \to h'X)/dp^3$ at large x and small p_T can now be written as

$$\sigma_A(h \to h') = \sum_k \left[\frac{\sum_{j_k} S_{hA}(j_k)}{\sum_{j_k} S_{hN}(j_k)}\right] \sigma_N{}^k(h \to h'). \quad (5)$$

$\sigma_N{}^k(h \to h')$ is the contribution to the nucleon cross section from a quark diagram with a final hadron h' that contains the leading quark(s) k and the summation over j_k extends over all such diagrams. For production of h' that contains only a single leading quark, e.g., $p \to \pi$, K, η, ρ, ω, φ, K^*, ..., or $\pi \to K$, π, η, ρ, ω, φ, K^*, ..., N, Σ, Λ, Ξ, ..., Eq. (5) leads, respectively, to

$$\sigma_A(p \to \pi, \ldots) = \frac{\sigma_{pA} - \sigma_{qA}}{\sigma_{pp} - \sigma_{qp}} \sigma_N(p \to \pi, \ldots), \quad (6a)$$

$$\sigma_A(\pi \to K, \ldots) = \frac{\sigma_{\pi A} - \sigma_{qA}}{\sigma_{\pi p} - \sigma_{qp}} \sigma_N(\pi \to K, \ldots). \quad (6b)$$

Equations (6) predict an A dependence which does not change with x.

Production of baryons that can contain two leading quarks like $p \to n$, Λ, Σ^0, ... can proceed via recombination of a single or two leading quarks, as indicated in Figs. 1(c)–1(e), and give rise to two terms with different A and x dependences,

$$\sigma_A(p \to \Lambda, \ldots) = \frac{\sigma_{pA} - \sigma_{\pi A}}{\sigma_{pp} - \sigma_{\pi p}} \sigma_N{}^2(p \to \Lambda, \ldots) + \frac{\sigma_{pA} - \sigma_{qA}}{\sigma_{pp} - \sigma_{qp}} \sigma_N{}^1(p \to \Lambda, \ldots). \quad (7)$$

Equation (7) can also be written as

$$\sigma_A(p \to \Lambda, \ldots) = \frac{\sigma_{pA} - \sigma_{\pi A}}{\sigma_{pp} - \sigma_{\pi p}} \sigma_N(p \to \Lambda, \ldots) + \frac{2\sigma_{\pi A} - \sigma_{pA} - \sigma_{qA}}{\sigma_{pp} - \sigma_{qp}} \sigma_N{}^1(p \to \Lambda, \ldots). \quad (8)$$

The second term on the right-hand side of Eq. (7) increases with A faster than the first term. However since the x distribution of a single valence quark is much steeper than that of a diquark, the relative importance of the second term increases when x decreases. This leads to a decreasing nuclear attenuation for smaller x values.

Nuclear attenuation of quarks can also be included in the quark-parton picture of deep-inelastic leptoproduction: The target quark that absorbs the virtual boson can either hadronize directly via recombination with target quarks, or first emit hadron fragments and then recombine. In both cases, if the observed hadron has a large fraction of the momentum of the virtual photon, the leading quark had to escape hard inelastic collisions with target nucleons. Nuclear matter is approximately transparent to photons and intermediate weak bosons, and their probability of striking a nuclear quark at (b,z) is proportional to the nuclear density $\rho(b,z)$. The probability of a quark struck at (b,z) escaping along the z direction is $\exp\{-\sigma_q \int_z^\infty \rho(b,z)dz\}$ and thus

$$\sigma_A(\gamma \to h, \ldots) = \sigma_N(\gamma \to h, \ldots) \int d^2b \int_{-\infty}^{\infty} \rho(b,z) \exp\{-\sigma_q \int_z^\infty \rho(b,z')dz'\} dz = (\sigma_{qA}/\sigma_{qN})\sigma_N(\gamma \to h, \ldots). \quad (9)$$

Equation (9) predicts an A dependence which does not change with x.

Experimental results on production from nuclear targets are often parametrized as

$$R_{a\to b}\left(\frac{A_2}{A_1}\right) \equiv \frac{\sigma_{A_2}(a \to b)}{\sigma_{A_1}(a \to b)} \approx \left(\frac{A_2}{A_1}\right)^{\alpha(x,p_T)}. \quad (10)$$

In our calculation of R and α, we used measured values[11] of σ_{pA} and $\sigma_{\pi A}$. σ_{qA} was calculated from Eq. (2) with $\sigma_q = 13$ mb and nuclear density functions that were determined by low-energy electron scattering.[12] In Fig. 2(a) we compare α predicted by (9) with α obtained from electroproduction of charged hadrons ($h^\pm$) by virtual photons[1] [$0.35 \leq q^2 \leq 5$ (GeV/c)^2 and $7 \leq s \leq 31$ GeV^2] on D, Be, C, Cu, and Sn targets. (Here, $-q^2$ is the square of the invariant mass of the virtual photon γ_v, and s is the square of the total energy in the $\gamma_v N$ c.m. system). The upper and lower lines in Fig. 2(a) are our predictions for Cu/D and Sn/D, respectively. They are in good agreement with experiment. In Fig. 2(b) we compare α as predicted by (6a) with α obtained from experimen-

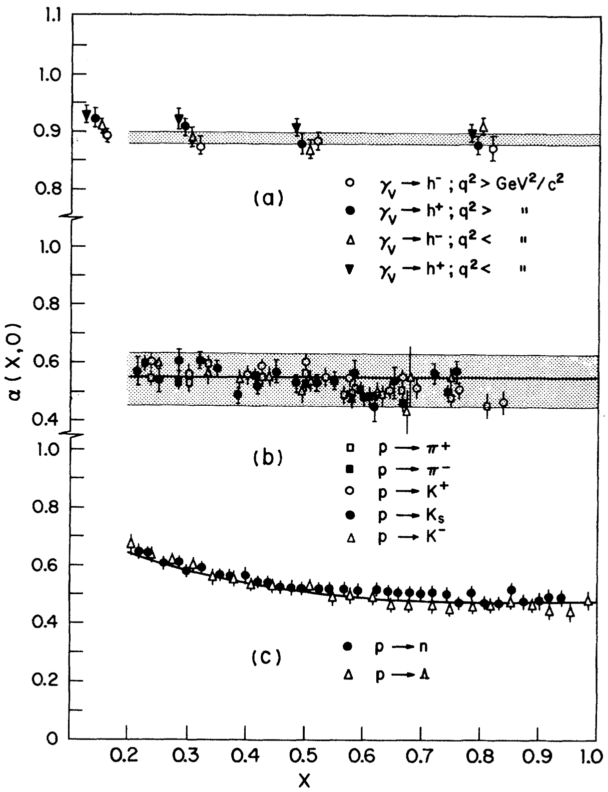

model predictions of $\alpha(x,\ 0)$ as defined in Eq. (10). (a) α from electroproduction of charged hadrons by virtual photons (Ref. 1). The upper and lower lines are, respectively, the predictions for Cu/D and for Pb/D. (b) α from $\pi^{\pm}$, $K^{\pm}$ production at $\theta = 17$ mrad by 19- and 24-GeV/c protons (Ref. 3) and from K_S production at 0° by 300-GeV/c protons (Ref. 2e). The line is the prediction for Pb/Be. The shaded area indicates the range of variation of the prediction for the different choices of A_1 and A_2. (c) $\alpha(x,\ 0)$ from Λ production by 300-GeV/c protons (Ref. 2b) and from n production by 400-GeV/c protons (Ref. 2c) at $\theta \lesssim 2$ mrad. The data points and the predictions are for Pb/Be.

tal data on $\pi^{\pm}$, $K^{\pm}$ production from Be, C, Al, Cu, and Pb targets at $\theta \cong 17$ mrad by 19- and 24-GeV/c proton beams[3] and from data on K_S production at $\theta \cong 0°$ from Be, Cu, and Pb targets by a 300-GeV/c proton beam.[2e] The line is our prediction for Pb/Be. The shaded area indicates the domain of variation of the predicted α for the different combinations of A_1 and A_2. The predictions are in good agreement with the experimental data. In Fig. 2(c) we compare α calculated from (8) with α obtained from experimental data on small-angle production of Λ by 300-GeV/c protons[2b] and of n by 400-GeV/c protons[13] from Be and Pb targets. In our calculations, we used $\sigma_N^{\,1}(p \to \Lambda \text{ or } n) = [0.73\ \text{mb}/(\text{GeV}^2/c^3)][u_p(x) + d_p(x)]$ with $u_p(x) = 2.1875(1-x)^3/\sqrt{x}$ and $d_p(x) = 1.2305(1-x)^4/\sqrt{x}$, and we assumed that $\sigma_{\text{Be}}(p \to \Lambda, n, \ldots) \cong (\sigma_{p\text{Be}} - \sigma_{\pi\text{Be}})\sigma_N(p \to \Lambda, n, \ldots)/\sigma_q$. Figure 2(c) demonstrates excellent agreement between theory and experiment.

We conclude that the quark picture of hadron and lepton collisions when it takes into account quark attenuation in nuclear matter provides a simple and accurate description of the A dependence of inclusive production of hadrons at medium and large x and small p_T.

The research reported here was supported in part by the U.S.-Israel Binational Science Foundation and by Yamada Science Foundation, Japan.

[a] Permanent address: Department of Physics, Tohoku University, Sendai 980, Japan.

[1] L. S. Osborne *et al.*, Phys. Rev. Lett. 40, 1624 (1978).

[2a] M. Binkley *et al.*, Phys. Rev. Lett. 37, 571 (1976).

[2b] K. Heller *et al.*, Phys. Rev. D 16, 2737 (1977).

[2c] D. Chaney *et al.*, Phys. Rev. Lett. 40, 71 (1978).

[2d] M. R. Whalley *et al.*, University of Michigan Report No. HE-78-46, 1979 (to be published).

[2e] P. L. Skubic, Ph.D. thesis, University of Michigan Report No. HE-72-32, 1973 (to be published).

[3] J. V. Allaby *et al.*, CERN Report No. 70-12, 1970 (unpublished); T. Eichten *et al.*, Nucl. Phys. B44, 333 (1972); S. A. Azimov *et al.*, Phys. Lett. 73B, 500 (1978).

[4] For quark recombination models see, for instance, H. Goldberg, Nucl. Phys. B44, 149 (1972); S. Pokorski and L. Van Hove, Acta Phys. Pol. B5, 229 (1974), and Nucl. Phys. B86, 243 (1975); L. Van Hove, Acta Phys. Austriaca, Suppl. 21, 621 (1979); W. Ochs, Nucl. Phys. B118, 397 (1977); K. P. Das and R. C. Hwa, Phys. Lett. 68B, 459 (1977); D. W. Duke and F. E. Taylor, Phys. Rev. D 17, 1788 (1978). For quark-interchange models see, for instance, S. J. Brodsky and J. F. Gunion, Phys. Rev. D 17, 848 (1978), and references therein. For quark fragmentation models see, for instance, R. D. Field and R. P. Feynman, Phys. Rev. D 15, 2590 (1977), and Nucl. Phys. B136, 1 (1978); H. Fukuda and C. Iso, Prog. Theor. Phys. 57, 483 (1977); O. Sawada, Prog. Theor. Phys. 58, 1815 (1977); B. Anderson *et al.*, Phys. Lett. 69B, 221 (1977), and Nucl. Phys. B135, 273 (1978); A. Capella *et al.*, Phys. Lett. 81B, 68 (1979).

[5] Many models of high-energy particle-nucleus interactions fail to predict the nuclear attenuation. See, for instance, A. Dar and J. Vary, Phys. Rev. D 6, 2412 (1972); K. Gottfried, Phys. Rev. Lett. 32, 957 (1974); S. J. Brodsky *et al.*, Phys. Rev. Lett. 39, 1120 (1977). Some models do predict nuclear attenuation but their predictions do not reproduce the experimental data. See, for instance, N. N. Nikolaev, Phys. Lett. 60B, 363 (1976); A. Capella and A. Kryzwicki, Phys. Lett.

67B, 84 (1977).

[6]A similar picture was independently suggested by N. N. Nikolaev and S. Pokorski, Phys. Lett. 80B, 290 (1979); N. N. Nikolaev and A. Ya. Ostapchuck, CERN Report No. TH-2575, 1978 (to be published). However, their model rests heavily on details of a specific quark recombination model, it is not applicable to lepton production, and their predictions involve a free choice of functions and adjustable parameters.

[7]We assume that quarks can propagate long distances through the nucleus as free quarks. We have not addressed ourselves to the problem of what is the mechanism that makes this possible, whereas confinement distances are believed to be of the order of nucleon dimensions. The answer to this problem has to wait first for the solution of the confinement problem.

[8]It is well known both theoretically (see, for instance, Ref. 6 and references therein) and experimentally (lack of significant cascading within nuclei) that formation times of large x particles are long compared with nuclear dimensions.

[9]G. Berlad *et al.*, Phys. Rev. D 13, 161 (1976), and references therein.

[10]E. M. Levin and L. L. Frankfurt, Pis'ma Zh. Eksp. Teor. Fiz. 2, 3105 (1965) [JETP Lett. 2, 108 (1965)]; H. J. Lipkin and F. Sheck, Phys. Rev. Lett. 16, 71 (1966).

[11]G. Belletini *et al.*, Nucl. Phys. 79, 609 (1966); S. P. Denisov *et al.*, Nucl. Phys. B61, 62 (1973); A. S. Carroll *et al.*, Phys. Lett. 80B, 319 (1979).

[12]S. Barshay *et al.*, Phys. Rev. C 11, 360 (1975).

[13]We used only the $\theta \neq 0°$ data of Walley *et al.*, Ref. 2d, to avoid the contribution from coherent production of resonances by the nuclear Coulomb field.

Dynamical Supersymmetries in Nuclei

F. Iachello

Department of Physics, Yale University, New Haven, Connecticut 06520, and Kernfysisch Versneller Instituut, 9700av Groningen, The Netherlands

(Received 16 January 1980)

It is suggested that dynamical (Bose-Fermi) supersymmetries may be present in the spectra of complex nuclei. A concrete example in which a supersymmetric structure is experimentally observed is shown. In this example the supersymmetry is generated by $L = 0$ and $L = 2$ bosons together with $j = \frac{3}{2}$ fermions.

In recent years, it has been pointed out by several authors that there may exist in nature examples of supersymmetric structures in which bosonic and fermionic degrees of freedom are linked together in a single theoretical framework.[1] However, no concrete example in which a supersymmetric structure is experimentally observed has been reported so far. In this Letter, I suggest that dynamical supersymmetries may be present in complex nuclear spectra and I show one concrete example where the supersymmetric structure is experimentally observed.

By analogy with an ordinary dynamical symmetry (which applies to a system either of bosons *or* of fermions separately), one can define a dynamical supersymmetry as that situation in which (i) the states of the combined system of bosons and fermions can be simultaneously classified with a complete set of group-theoretical labels; (ii) these states are split but not mixed by the Hamiltonian, H, and (iii) the *same* expression for the eigenvalues of the system in terms of the complete set of group-theoretical labels described *both* bosonic and fermionic spectra.

The investigation of this problem was stimulated in part by the fact that similar attempts have been made in elementary-particle physics and in part by the known occurrence of several ordinary dynamical symmetries in the spectra of complex nuclei.[2] In particular, the spectra of the platinum nuclei with an even number of protons and neutrons have been shown to display a dynamical symmetry associated with the group O(6).[3] The states of these nuclei have then been classified by the set of labels related to the group chain[4] $U(6) \supset O(6) \supset O(5) \supset O(3) \supset O(2)$, denoted by N, σ, τ, ν_Δ, L, and M. The group U(6) and its subgroups are generated by $L = 0$ and $L = 2$ bosons. In terms of these labels, the expectation value of the most general Hamiltonian which splits but does not mix the states can be written as[4]

$$E(N, \sigma, \tau, \nu_\Delta, L, M) = -\tfrac{1}{4}A\sigma(\sigma+4) + \tfrac{1}{6}B\tau(\tau+3) + CL(L+1), \quad (1)$$

where, in comparison with Eq. (12) of Ref. 4, the constant $\frac{1}{4}AN(N+4)$ has been removed, since it does not contribute to the excitation energies. An ordinary symmetry associated with the group chain $O(6) \supset O(5) \supset O(3)$ is then present whenever